# Correlative visualization techniques for multidimensional data

by L. A. Treinish C. Goettsche

Critical to the understanding of data is the ability to provide pictorial or visual representations of those data, particularly in support of correlative data analysis. Despite the many advances in visualization techniques for scientific data over the last several years, there are still significant problems in bringing today's hardware and software technology into the hands of the typical scientist. For example, there are computer science domains other than computer graphics, such as data management, that are required to make visualization effective. Well-defined. flexible mechanisms for data access and management must be combined with rendering algorithms, data transformations, etc. to form a generic visualization pipeline. A generalized approach to data visualization is critical for the correlative analysis of distinct, complex, multidimensional data sets in the space and earth sciences. Different classes of data representation techniques must be used within such a framework, which can range from simple, static two- and three-dimensional line plots to animation, surface rendering, and volumetric imaging. Static examples of actual data analyses will illustrate the importance of an effective pipeline in a data visualization system.

#### Introduction

The importance of data visualization, where visualization means those methods of computing that give visual form to complex data by utilizing graphics and imaging technology, has been recognized for some time. Only recently, however, has it begun to grow in importance among the scientific community in general. This concept has been particularly relevant for analyzing large volumes of complex (e.g., multidimensional) data streams that are available today from such sources as spacecraft instruments and supercomputer-based models and simulations. The human visual system has an enormous capacity for receiving and interpreting data efficiently. Hence, the processing power of the eye-brain system should be an intimate part of any effort to comprehend data [1]. Unfortunately, such data are often generated today without adequate consideration of the difficulty involved in their effective interpretation (i.e., extracting useful knowledge from data). This problem will be compounded by the next generation of data sources, which will literally bury the scientific community in bits. For example, NASA's Earth Observing System, which is planned for deployment in the late 1990s, will have to receive, process, and store one to ten terabytes (10<sup>12</sup> to 10<sup>13</sup> bytes) of data per day.

Despite advances in data generation and computer technology over the last few decades, methods of

<sup>©</sup>Copyright 1991 by International Business Machines Corporation. Copying in printed form for private use is permitted without payment of royalty provided that (1) each reproduction is done without alteration and (2) the Journal reference and IBM copyright notice are included on the first page. The title and abstract, but no other portions, of this paper may be copied or distributed royalty free without further permission by computer-based and other information-service systems. Permission to republish any other portion of this paper must be obtained from the Editor.

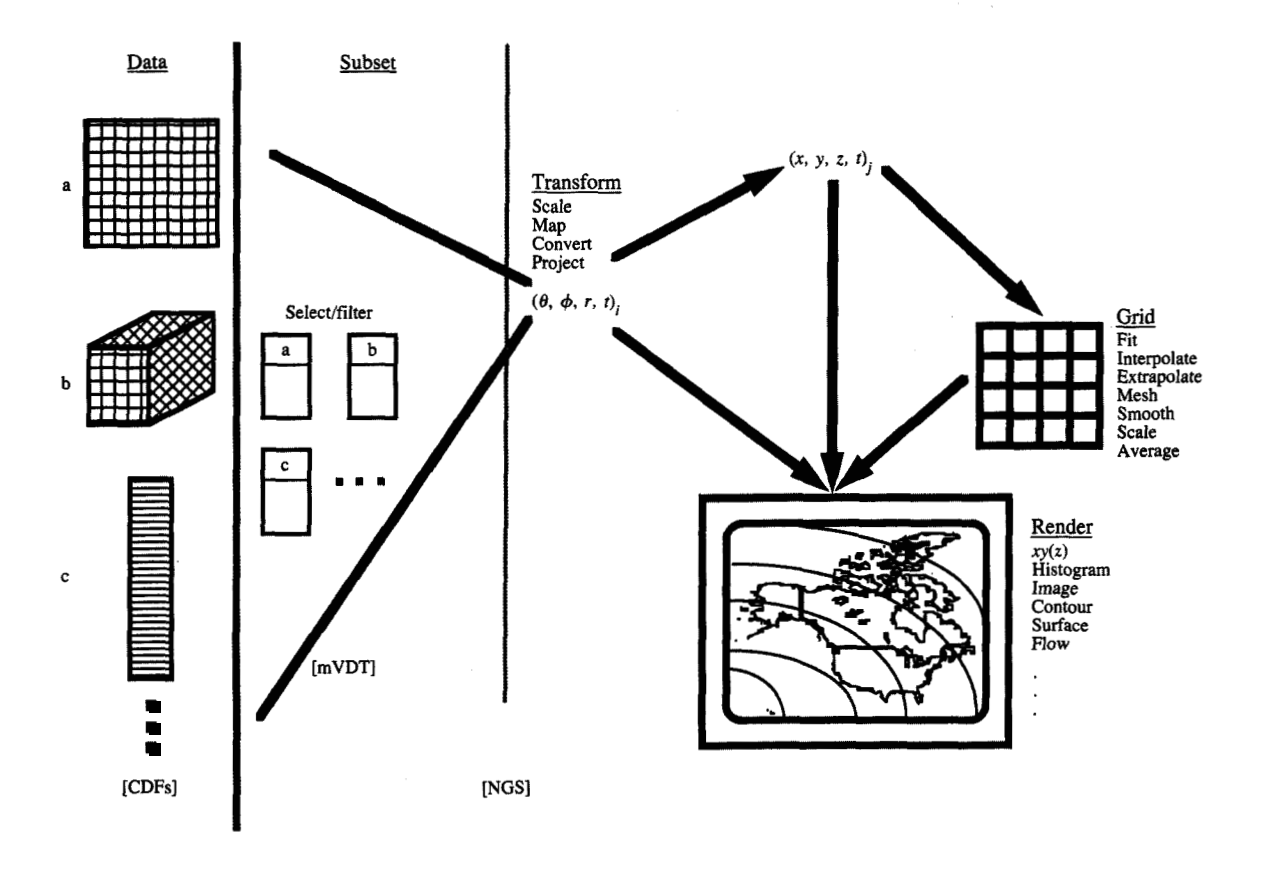
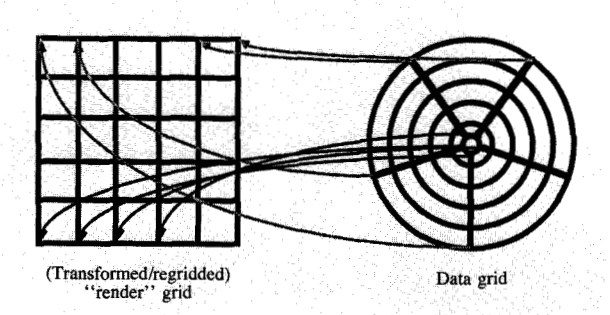


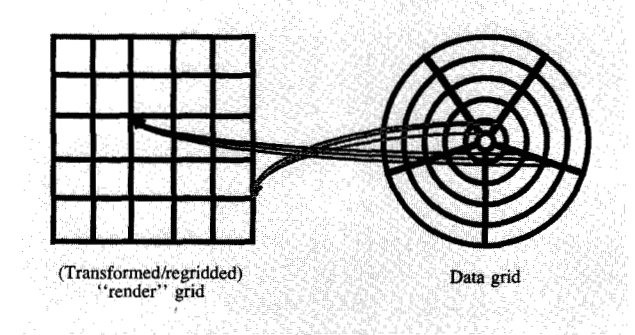
Figure 1

Effective generic visualization pipeline.

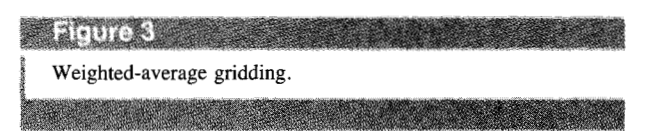
managing and analyzing large volumes of complex data streams have not basically changed. Potentially, this situation leaves significant fractions of data not fully understood, and scientific information undiscovered. Even with the availability of visualization technology as one very valuable technique in the study and analysis of large volumes of data, the importance of the organization, structure, and management of such data and associated information about data or metadata must be stressed. Without such considerations, a user would be unable to take advantage of powerful visualization tools for arbitrary data of interest—to see the unseen. The advent of powerful, relational database management systems (RDBMS), which have become commercially viable over the last few years, only begins to address these problems. Unfortunately, RDBMS technologies generally have been practical only for metadata management in large, scientific applications [2, 3].

Nevertheless, a mechanism is still required for organizing the actual data, which may be complex, large in volume, and resident on magnetic disk. Such data can be referenced by a RDBMS, but data management capabilities are still required at the applications level for the actual data. Such a data (base) model must be matched to the structure and use of scientific data. One such mechanism is the Common Data Format (CDF). It is based upon the concept of providing data-independent, abstract support for a class of scientific data that can be described by a multidimensional block structure. It has been used to develop a number of generic data management, display, and analysis tools for a wide variety of disciplines. Users of data-independent application systems, which are based upon CDF, rely on their own understanding of the science behind different sets of data to interpret the results, a critical feature for the multidisciplinary studies inherent in the space and





# Figure 2 Nearest-neighbor gridding.



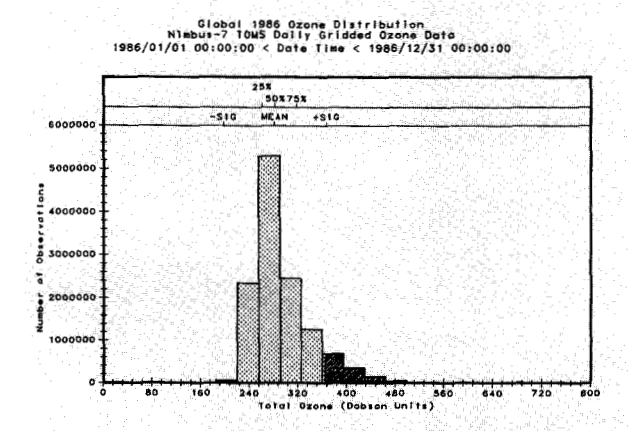


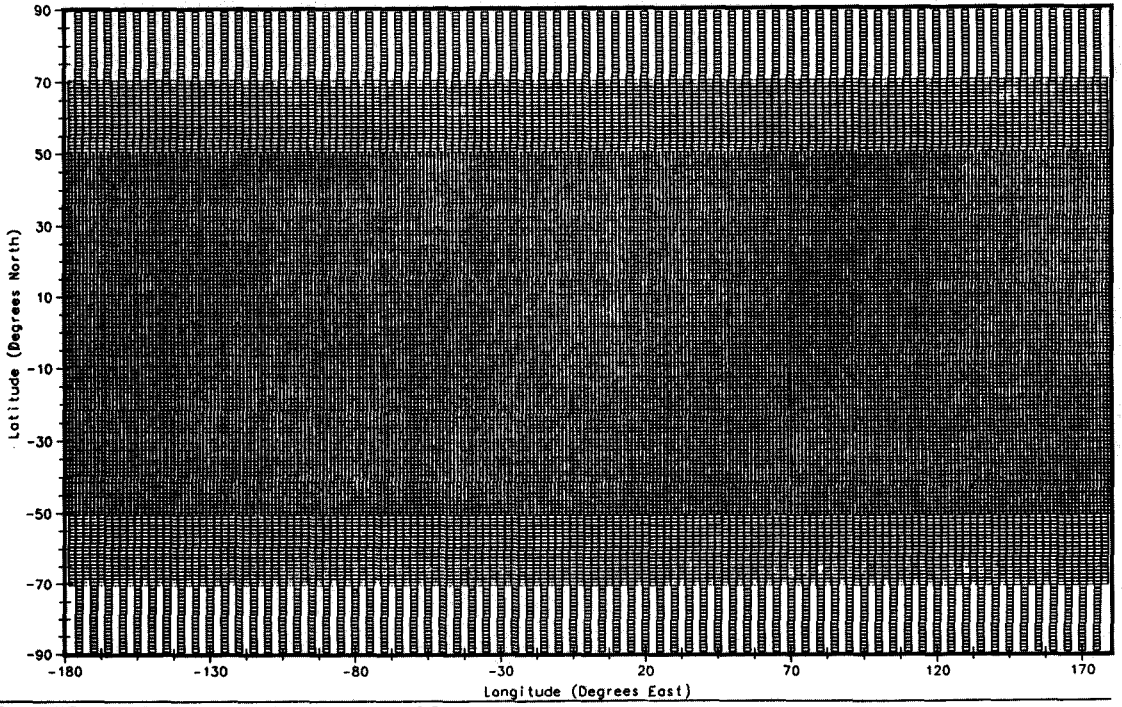
# Figure 4 Statistical distribution of Nimbus-7 global total ozone for 1986.

earth sciences [4]. CDF has become a standard method for storing data in these disciplines for a variety of applications. This abstraction consists of a software package and a self-describing data structure. The term "data abstraction" implies that CDF isolates the details of the physical structure of a data set from a user of such data [5]. The programmer using such an abstraction needs to know only about the collection of CDF operations and the logical organization of the data of interest, not the details of CDF storage or the underlying software structure. Therefore, CDF easily accommodates scientific data structures at the applications-programmer level rather than at the physical data level.

#### Effective visualization

A researcher's employment of tools to visualize data is an important mechanism in the data analysis process. In view of this, how does a scientist-user access data of interest and the appropriate visualization tools in a reasonable, acceptable manner? Most of the visualization software technology available today is *not* in a form that permits straightforward application to data of interest without significant assistance from experts. There are a plethora of graphics and imaging toolkits available from a variety of sources. Some of these toolkits are standards, while others are proprietary (recent packages, such as PHIGS+, RenderMan, Wavefront, CubeTool, and Doré or older examples, like DISSPLA, Template, SAS, and MOVIE.BYU, a few of which are surveyed in [6]). However, as powerful as these software packages may be, they are, unfortunately, just boxes of tools, often only at a subroutine library level. The result is that such software is either unavailable to or unusable by the average scientist without significant graphics expertise. These software toolkits are typically not "turnkey" in nature, have no mechanism for handling discipline- or domaindriven problems or data, lack a standard or intuitive interface above a programming language level, and so forth. Most so-called visualization systems do not deal directly with science problems but rather are oriented toward graphics and animation (i.e., points, vectors, polygons, bitmaps, voxels, lighting models, animation, etc. are addressed rather than multispectral images, geographic grids, electromagnetic tensor fields, atmospheric sounding, time histories, etc.) [1, 7, 8].

Given the demands of modern research, scientists who are not computer-oriented rarely have the time or the interest to learn graphics protocols and standards, data structures, peculiarities of specific devices, rendering October 1986 South Pole Ozone Hole Nimbus-7 TOMS Daily Gridded Ozone Data 1986/10/10 00:00:00 < Date Time < 1986/10/10 00:00:00



FILTER: 10.00 <= IDAY <= 10.00

#### 37.77 E

Spatial distribution for Nimbus-7 TOMS grids.

algorithms, etc., all of which are often required in order to use typical "visualization" toolkits. They can witness the substantial achievement represented by the class of scientific visualizations created by computer hardware and software vendors, supercomputer centers, and government research laboratories. However, such examples are often customized for specific applications, involve considerable intensive work by visualization specialists, and are essentially unavailable to the typical scientist in most disciplines, beyond the acquisition of a copy on videotape. If, as computer graphics specialists claim, visualization is to be truly effective, if not revolutionary, for use by scientists in their routine research, the technology must be interactive and must operate on the scientist's terms, not on those of an arcane collection of software tools.

# • Science requirements

The support of correlative data analysis (i.e., working with data from a variety of sources to study a problem of

scientific interest) requires an obvious focus on generic visualization via the development of discipline-independent visualization techniques. This implies the ability to examine many different parameters from disparate data sets in the same fashion for visual correlation, a function well-suited to the capabilities of the human visual system. However, there must also be many common visualization schemes, so that any one set of parameters can be studied through different mechanisms, because not all visualization techniques show all aspects of the data. Such visualization functionality must be available at a high level, with a consistent user interface enabling the scientist to easily access the full capability of the software.

Therefore, discipline-independent visualization implies the development of software that handles arbitrary data sets and possesses different tools for displaying data. In other words, data management is as important a component of a data visualization system as underlying graphics and imaging technology. To implement a system

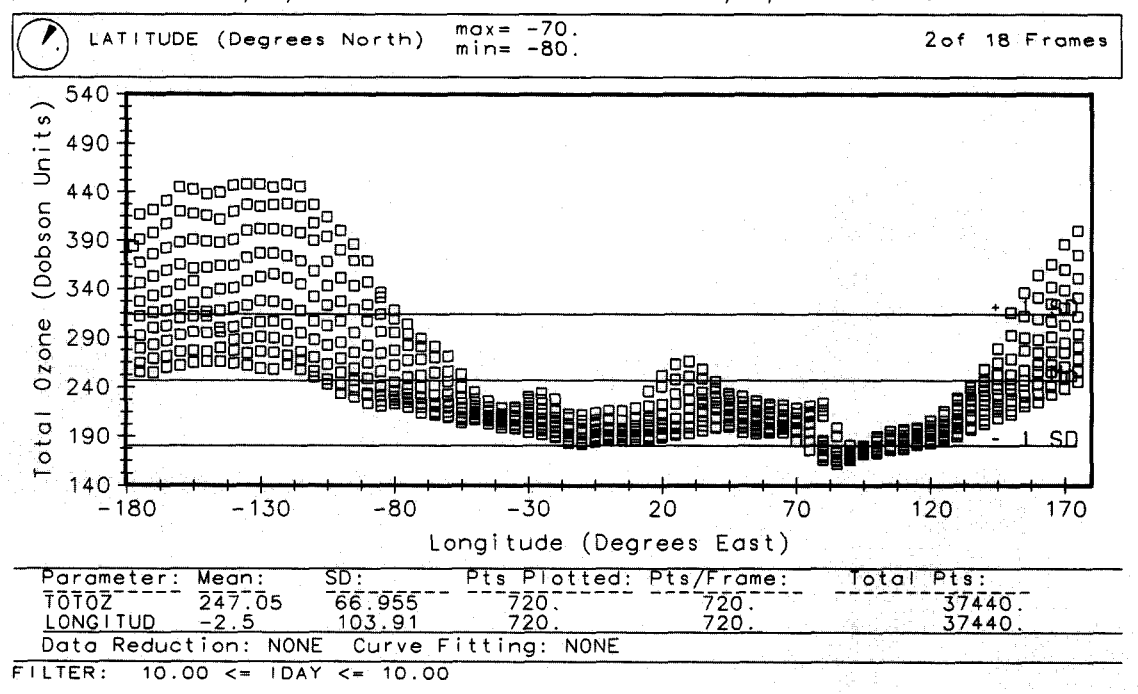


# Figure 6

Meridional distribution of TOMS total ozone from  $-70^{\circ}$  to  $-80^{\circ}$  latitude on October 10, 1986

that provides these features in a practical fashion, the management of and access to the data must be decoupled from the actual visualization software. Within such a system, there must be a clean interface between the data and the display of the data so that arbitrary data can be accessed by the visualization software. In other words, an appropriate data model is needed that accommodates the access and structure of scientific data on one hand and the requirements of visualization software on the other. CDF is one example of such a data model. In addition, a common intuitive user interface for the selection of techniques for data presentation and manipulation is required. As a consequence of such an approach, a software system of this design has an open framework. It can ingest arbitrary data objects for visualization, and other visualization techniques can be added that are independent of the application. These abilities imply a significant reduction in long-term software development costs, because new data sets do not require new display software and new display techniques do not require new data access software.

The NSSDC (National Space Science Data Center) Graphics System (NGS), for example, provides an interactive, discipline-independent toolbox for nonprogrammers to support the visualization of data. In order to utilize the NGS, data of interest must be stored in terms of the aforementioned Common Data Format (CDF). The NGS supports the ability to display or visualize any arbitrary, multidimensional subset of any data set by providing a large variety of different representation schemes, all of which are supported by implicit animation (i.e., slicing of a data set into sequences). Treinish [9] discusses the basic design, interface, implementation, and applications of the NGS. So as not to duplicate that material, the following sections elaborate on the underlying architecture of visualization software, and how visualization techniques should be used to support correlative data analysis. These discussions do apply to the NGS but are not covered in [9].

# Visualization pipeline

Generic data visualization implies the geometric or visual representation of arbitrary, multidimensional data from a variety of sources or disciplines. Given well-defined, flexible mechanisms for data access and management,



Figure 7

Total global ozone on October 10, 1986, on a Cartesian map.

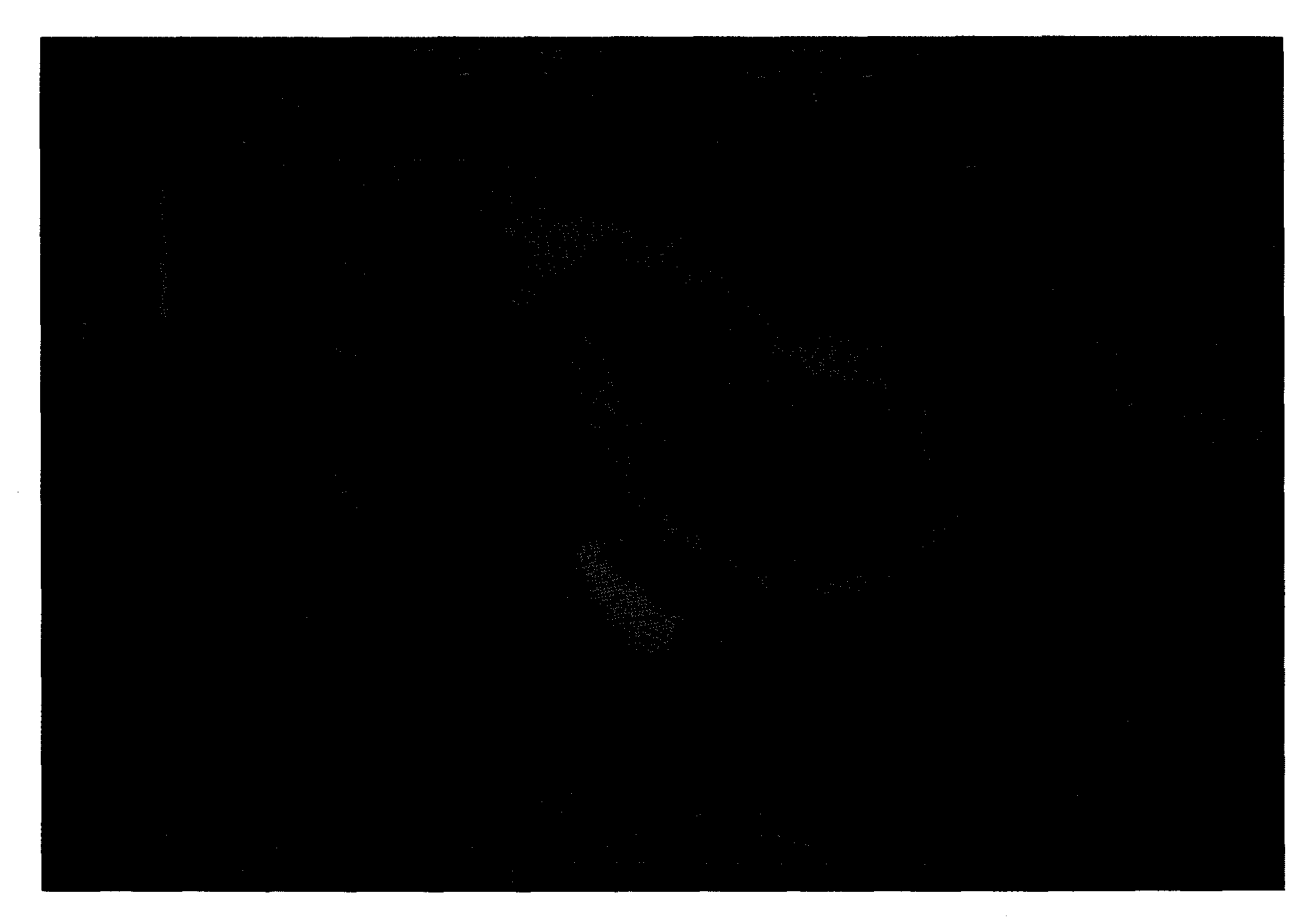
there exist specific rendering algorithms, data transformations, etc. that can be cast into a generic framework when they are part of a visualization pipeline. A generalized approach to data visualization is very valuable for the correlative analysis of distinct, complex, multidimensional data sets in the space and earth sciences. Different classes of data representation techniques are required, since they each may show different aspects of data. Such techniques may range from simple, static two- and three-dimensional line plots to animation, surface rendering, and volumetric imaging. Only some of these techniques may be relevant for specific data sets. Hence, a wide variety of representation schemes are necessary to accommodate a disparate collection of data. The key is a basic structure—the visualization pipeline—for generic visualization, which permits the scientist-user to control the flow of data under study and promotes exploratory data analysis.

Figure 1 is a schematic for a visualization pipeline that meets the above requirements. The implementation of such a pipeline must be under a uniform interface to

permit consistent user access to each portion thereof. The interface supports the ability to move data through the pipeline interactively to foster visual analysis. It provides a virtual view of the pipeline. Such a structure permits an iterative invocation of each function on demand. Of course, for the pipeline to be effective, these functions must be accessible at a scientific level.

# Data selection

On the left side of Figure 1, the data management portion is shown schematically. It provides the capability to select data sets of interest. In an end-to-end data system this management kernel may vary from traditional data catalogs and inventories to a highly interactive, intelligent information system with imbedded semantics. In either case, tools are provided, at some level, to help a user understand and select appropriate data sets. For example, correlative data analysis may require the selection of several "parallel" data sets of potentially different structures (e.g., one or more CDFs). This data management capability is required as the data



Four 8

Spatial distribution of ozone over the Southern Hemisphere on October 10, 1986.

flow to the right in the diagram, in which the data are divided into subsets. From the chosen data sets a user may select only those variables or parameters of interest. Optionally, only a portion of the selected domain of the parameters may be required. Therefore, the capability to window or filter out the undesired section(s) of the data set(s) is needed.

### • Transformation

The next portion of the pipeline deals with manipulating the data to meet the requirements of the analysis. For example, if the data chosen are not in the desired form for display or do not match the required form for the rendering method, the data must be reorganized. This implies operations such as rescaling, mapping to another coordinate system, converting the units, and projecting the data geographically. If, however, the data are already in the form required for display, no transformation is required.

#### • Gridding

If the rendering method is for continuous data and the data are not continuous, a uniform grid must be created at some desired resolution. This requirement also arises from gridded data that have been transformed into a nonuniform grid or from data accessed from multiple sources with dissimilar grid resolutions. In either case, operations such as curve and surface fitting, meshing, kriging, interpolation, smoothing, scaling, and averaging are required. However, if the data are already in a uniform grid at the desired resolution (e.g., a simple image), the data may be rendered as they are.

Figures 2 and 3 illustrate examples of simple gridding schemes which are an important part of a visualization pipeline and are among the techniques available in the NGS. Figure 2 shows the concept behind nearestneighbor gridding, in which the cells of a grid are populated by extracting values from the points in the original grid which are spatially nearest. Such a technique

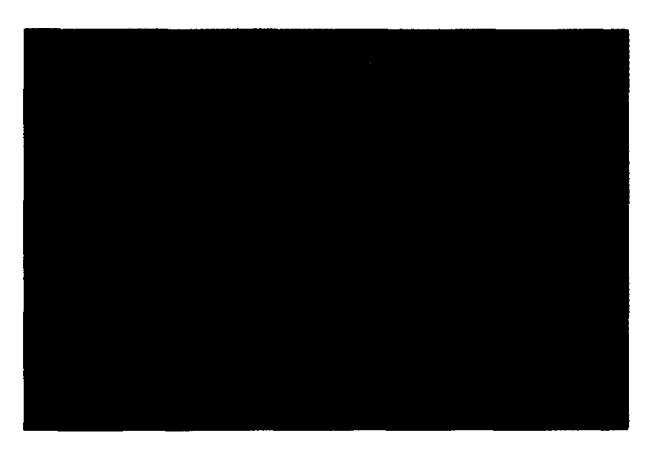


# Figure 9

Simple contour map of ozone over the Southern Hemisphere on October 10, 1986.



# Fairs 10

Simple mapped pseudo-color image of ozone over the Southern Hemisphere on October 10, 1986.

is valuable because it preserves the original data values and distribution of a grid after a coordinate transformation may have taken place on a collection of points. In addition, it is computationally inexpensive.

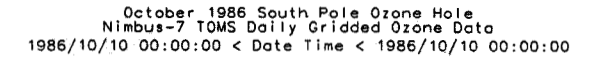
Figure 3 shows the concept behind weighted-average gridding, in which, for any given cell in a grid, the weighted average of the n nearest values in the original data distribution (grid or collection of points) spatially nearest to that cell has been chosen. The selection of points is done only after any required coordinate transformation has been performed. A weighting factor,  $w_i = f(d_i)$ , where  $d_i$  is the distance between the cell and the ith  $(i = 1, \dots, m)$  point in the original grid structure after any transformation, is applied to each of the n values. Figure 3 illustrates the case where n = 3, which is utilized in the NGS along with  $w = d^{-2}$ . See [10, 11] for further discussions of this class of gridding algorithms.

#### Rendering

The result of any data selection or manipulation within this visualization pipeline is the actual data display. A user may choose one or more visualization primitives ("VPs"), which are inherently mapped to the dimensionality of the data to be displayed. A VP is a member of a class of primitives based upon some geometry (e.g., vector, polygon, raster/pixel, volume/voxel). Within each geometric class exists a collection of VPs. For example, vector- and polygon-based primitives can be divided into two subclasses: discrete (e.g., xy[z], two- and three-dimensional histograms) and continuous (e.g., two- and three-dimensional surfaces meshes, two- and three-dimensional field flows). The

implementation of each VP within the visualization pipeline can be decomposed into two portions, geometric modeling and the actual rendering. Such a decomposition maximizes the flexibility to operate on a variety of data streams. However, for this technique to be effective from the user perspective, the user must have some control over the presentation of data. Some of this authority may be as mundane as annotation, but it is critical for a posteriori interpretation of a visualization. The visualization pipeline, through its user interface, provides the ability to choose from a suite of VPs, while the underlying modeling and rendering software is hidden. Other presentation control factors may be specific to a single VP (e.g., the selection of the intervals between contour lines). The user must have the capability to assign any of the parameters in the data set to any of the (virtual) axes consistent with a specific VP. In addition, animation as a sequencing of frames according to a variable that has been mapped to an "animation axis" is critical.

For example, the generic rendering of shaded surfaces from multidimensional data sets within this pipeline is particularly challenging. The decoupling of the rendering process from the prerequisite geometric modeling permits a user to choose a general geometric model of a three-dimensional surface (e.g., sphere, parallelepiped) for a data stream of interest. This is as simple as global topography represented as data streams of latitude, longitude, and height above sea level, which are then mapped onto a spherical model. Such surfaces can then be independently rendered as wire-frame or smooth-shaded surfaces on typical workstations with hardware support for three-dimensional graphics. In addition, static images of surfaces with high-quality (Phong or ray-traced) shading can be generated by software renderers.



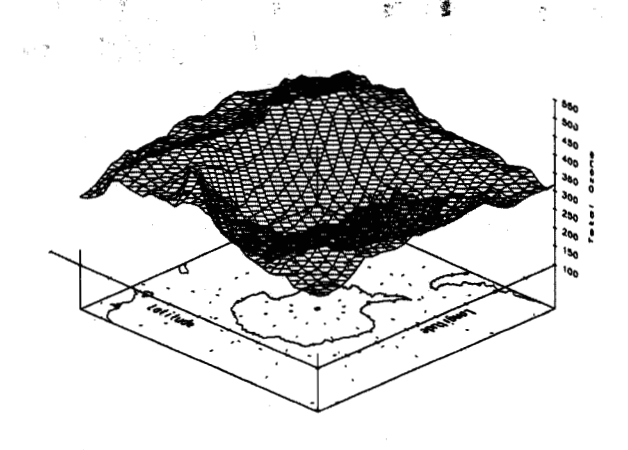


# Figure 11

Simple mapped surface mesh of ozone over the Southern Hemisphere on October 10, 1986.

Options associated with this class of visualization primitives are the use of pseudo-color for overlays of a data stream and animation for sequences of such models as described above. The pseudo-color, which maps a continuous color spectrum to a scaled quantitative range of values, can represent the same data stream as the "third" dimension, and hence act as a depth-cueing device in viewing the model. Alternatively, the pseudocolor can represent a "fourth" dimension, which, in the case of the topographic data, can be, for example, temperature as a function of latitude and longitude. Animation sequences can show the changes in all data streams (i.e., up to four) from one model to the next with respect to some other variable within the selected data set(s) (e.g., time). Although such a progression of animation frames is independent of the original data structures and display hardware, current workstation technology with support for three-dimensional graphics can accept sequences derived from disparate data sets and display them in real time.

#### Support

The components of the visualization pipeline require additional support in operational environments through optional features. As discussed earlier, the user must have control over the presentation of visualization primitives operating on data. However, such influence must extend to that portion of the pipeline between data selection and rendering, data transformation and gridding. Under

transformation, the key area is the ability to deal with different coordinate systems and to be able to transform data among them (e.g., Cartesian and polar in two dimensions; and Cartesian, spherical, and cylindrical in three dimensions). An important subclass of such transformations pertains to geographic mapping. Obviously, an effective visualization system for earth scientists must be capable of displaying data geographically through a variety of map projections (e.g., Mercator, stereographic). Such functionality, however, must be very flexible. A user must be able to select an appropriate projection (i.e., to flatten the earth) to preserve, for example, distance or shape; to choose an arbitrary geographic window to view the data with a map overlay of desired resolution; and to invoke such mapping with any visualization primitive. These characteristics of different map projections have been used by cartographers for centuries [12]. The ability to map any data to a particular geographic projection is also important for correlative analysis. By selecting the specific projection, the viewing vector and a magnification factor, a variety of data can be studied over the exact same geographic region within a consistent visual domain. Such generic geographic registration is not bound to any particular data stream. Since this class of coordinate system transformations really applies to any visualization of data on a spherical surface, the mapping functionality should also be available for data that are not located on the earth. (See [13] for a discussion of a geographic mapping package and applications of map projections.)

The second area of support applies to data manipulation in the gridding and transformation portions of the pipeline. The user must be able to select easily (and understand) the specific algorithms for reorganizing data flowing through the pipeline in order to choose different techniques for exploring the implications of such data manipulations. These abilities include choices such as polynomial vs. cubic spline curve fitting, nearest-neighbor selection vs. averaging for meshing, and linear vs. quadratic interpolation. A corollary to such an approach is the ability to handle point and continuous data in the same fashion. Hence, a user can grid a collection of points and render them as a continuous data set, or decompose a continuous data set into a collection of points and display them using a discrete visualization primitive. This method is very valuable for visual data correlation, for example, when trying to compare ground truth (point data) with spacecraft imagery (continuous data).

In the gridding as well as the rendering portions of the pipeline, a problem often occurs when specific techniques are applied to large data sets. Gridding algorithms, such as the ones discussed earlier, typically require searching

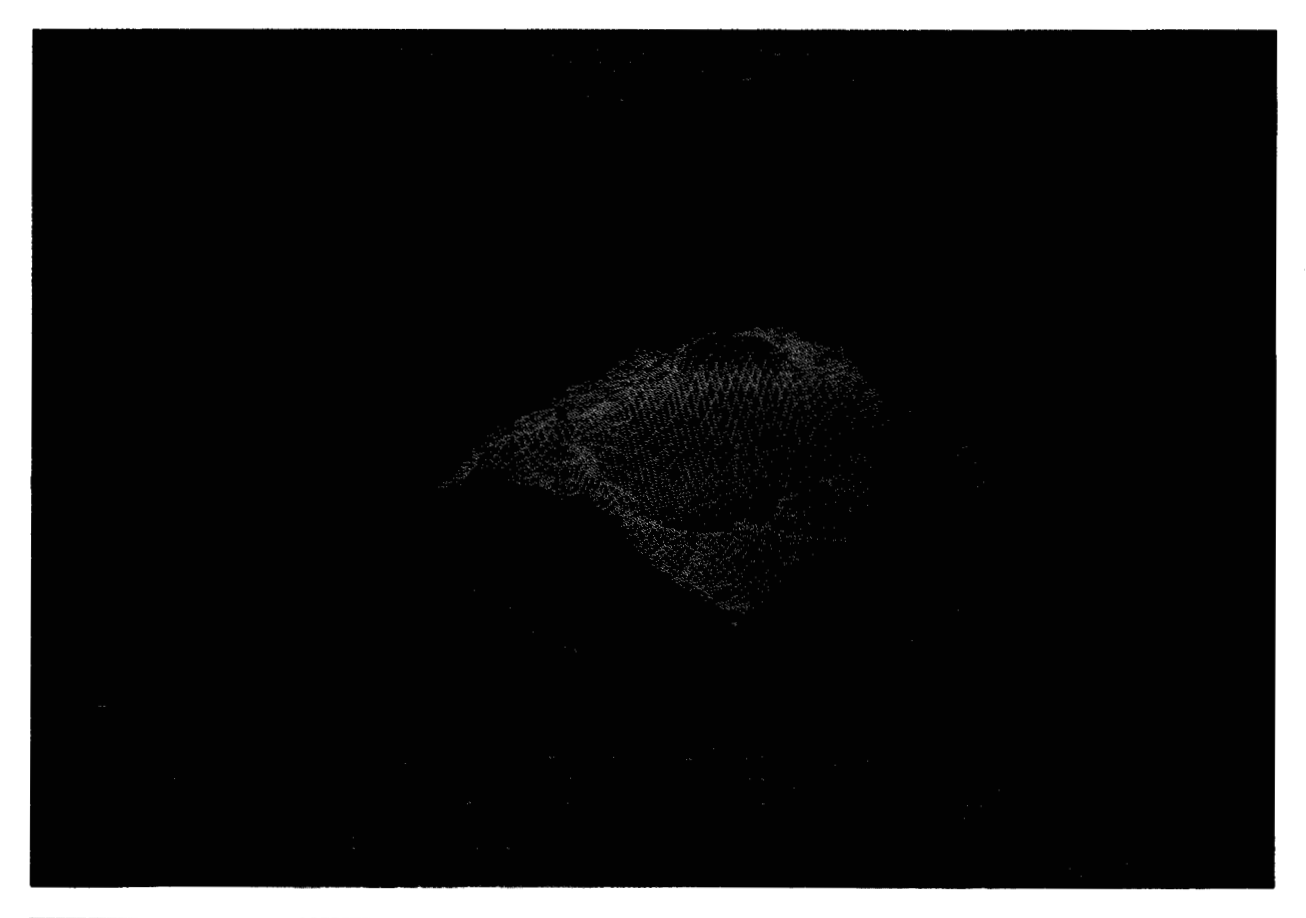


Figure 12

Mapped shaded surface mesh of ozone over the Southern Hemisphere on October 10, 1986.

through an entire data set. If the data set is large, the selection of a data subset that is also large via a simple linear search becomes prohibitively expensive. The computation time for such a search typically increases as  $n^2$ , where n is related to the number of points being examined. Very useful in alleviating this problem are hierarchical data structures, for which the overhead to generate the appropriate tree structure for the data set is justified when the number of data points is sufficiently large [14, 15].

For example, the storage and sampling of large, three-dimensional (e.g., geographic) data sets are improved by placing the data in an octree. Data values can be located by latitude and longitude within the octree structure, which supports fast retrieval. In addition, the octree assists the calculation of data for any given (geographic) location, which is accomplished by rapidly examining the actual data near the specified location and deriving a value via a specific gridding or interpolation algorithm. This technique can be valuable for correlating data by providing a consistent geographic reference among data

sets that are of different resolutions or are not geographically registered.

Octrees can also be used to build a spherical surface model as a geodesic sphere, for which further subdivision implies a more refined model at greater computational expense. For the display of cell arrays (e.g., pseudo-color images via vector/polygon protocols), quadtree-based rectangular subdivision compresses the number of cells (i.e., polygons) that actually are transmitted to a device. This process reduces transmission and rendering time because contiguous areas of similar data classification are combined to form one graphics primitive. The NGS uses this technique to support displays of high-resolution pseudo-color imagery on simple color graphics devices accessible via low-bandwidth communications.

# **Examples**

The NSSDC Graphics System (NGS) represents a prototype implementation of a generic visualization pipeline. Its effectiveness has been demonstrated by its operational use to support scientific research in a number

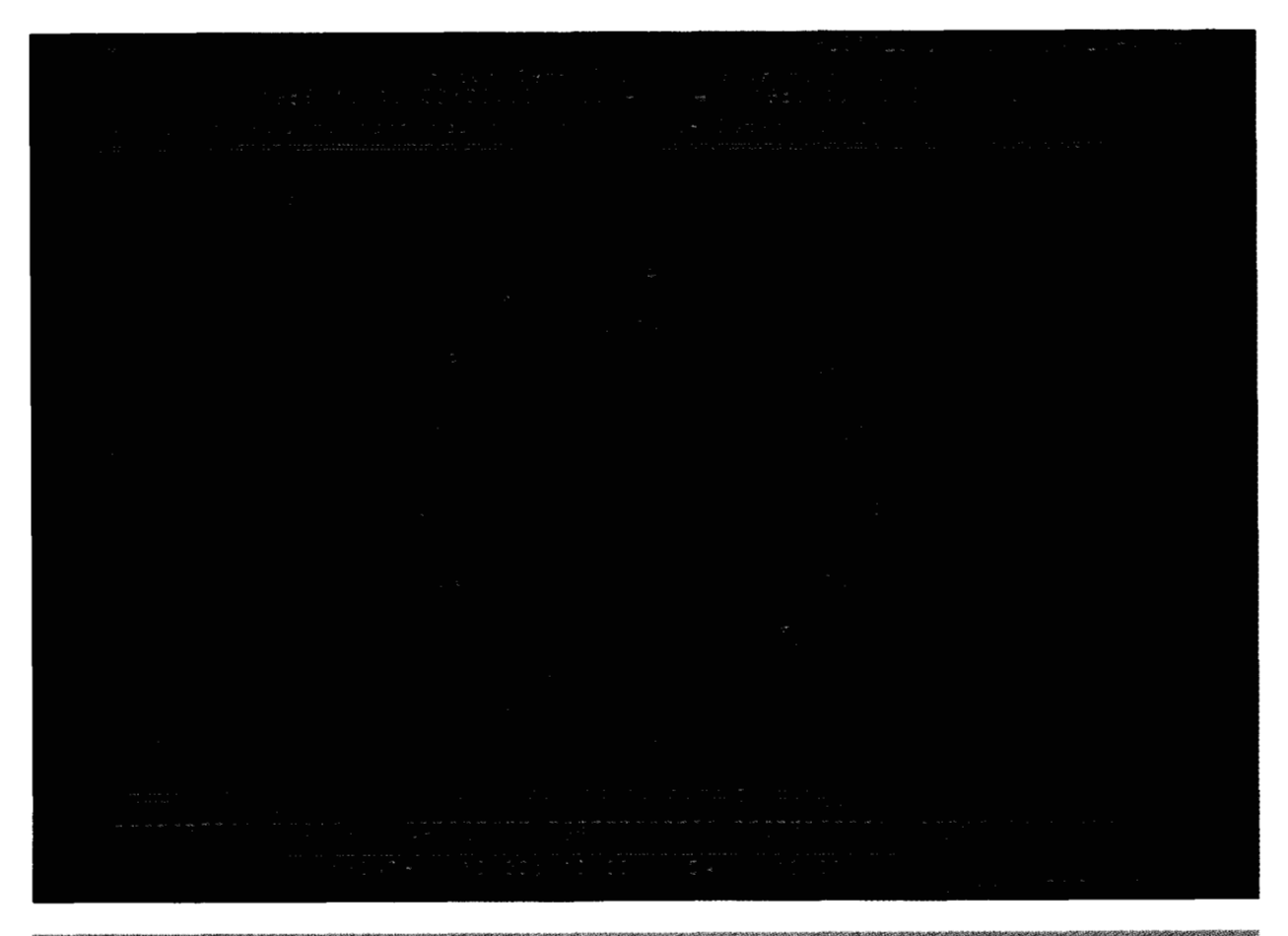


Figure 13

Optimized contour map of total ozone over Antarctica on October 10, 1986.

of disciplines. To illustrate the discussion of the pipeline in the previous section, a number of examples follow. These examples have been generated by controlling the flow of data through the NGS's implementation of the pipeline and the presentation of the data through different visualization primitives. This collection of visualizations can serve as an assessment of the uses of a visualization pipeline to correlate and study complex data. It also illustrates the importance of supporting many visualization techniques and the need for iterative display in the exploratory data analysis process. Such functionality can be critical for the study of observational data sets as opposed to simulations or computational models. Artifacts of the observation process (e.g., data gaps, orbital footprints, sensor resolution, instrument degradation, etc.) must be accommodated and compensated for in data visualization.

All of the examples were generated on a DEC VAX\* 8650 processor under VMS at the NSSDC using a

number of different graphics devices. Figures 4 through 14 and 22 through 26 were generated by the use of a commercial graphics package, Template, developed by TGS, Inc. of San Diego, which the NGS employs for the underlying graphics environment and device support. The other figures utilized hardware-specific and locally developed software. Treinish [9] discusses the implementation of the NGS and offers sample visualizations from a number of different disciplines.

A data set of current public and scientific interest is derived from the Total Ozone Mapping Spectrometer (TOMS) on board NASA's Nimbus-7 spacecraft.

Observations from TOMS have been invaluable to scientists studying the global distribution of ozone. The key data set from TOMS is in the form of daily world grids and is archived at the NSSDC from late 1978 through the present. In fact, the entire data set resides on line in CDF because of its importance to the scientific community. These data have become increasingly valuable because they indicate the presence of the so-

<sup>\*</sup> VAX is a trademark of Digital Equipment Corporation.



Optimized mapped pseudo-color image of ozone over the Southern Hemisphere on October 10, 1986.

called ozone hole over the South Pole, which is the result of the reduction in total ozone observed during the Antarctic spring in recent years. The total ozone content as derived from the TOMS observations is indicated in terms of Dobson units in the subsequent figures; 100 Dobson units are equivalent to a one-millimeter column of ozone at standard temperature and pressure. These gridded TOMS data are provided in their own unique nonuniform grid (37440 cells per grid) over the earth. For latitude the values are in degrees north (-90° to +90°). For longitude the grid values are in degrees east  $(-180^{\circ} \text{ to } +180^{\circ})$ . All 37440 cells in each of these grids imply a cell size of 1.0 degree in latitude, pole to pole. The nonuniformity of the grid in longitude is such that for latitudes (north and south) between the equator and 50° the longitude cell size is 1.25°; for latitudes between 50° and 70°, the longitude cell size is 2.5°; and for latitudes above 70°, the longitude cell size is 5° [16]. Hence, the tools of the NGS visualization pipeline provide a mechanism for analyzing the data that is independent of the limitations of the specific structure of the original data.

For the purpose of this sample study, the analysis of ozone data from 1986 has been selected. Figure 4 is a simple histogram derived from all of the points in the gridded data set for 1986 (about  $13.7 \pm 10^6$  points). The NGS pipeline allows the TOMS data set to be treated as essentially dimensionless or flat for the preparation of statistical summaries such as histograms. The number of times a total ozone value occurs in Dobson units within the illustrated collection of total ozone bins is shown along with the mean and standard deviations and percentile levels.

To study the ozone hole in more detail, one can continue to use the left-hand portion of the visualization pipeline (as shown in Figure 1) to select a specific subset of the TOMS data set beyond simply selecting the year, 1986. Although the following examples are static and emphasize techniques primarily for the study of the spatial characteristics of the data, time can be used for one of the virtual axes in the pipeline, including animation. October 10, 1986 has been chosen for further study because of the depth of the Antarctic ozone hole on that particular day.

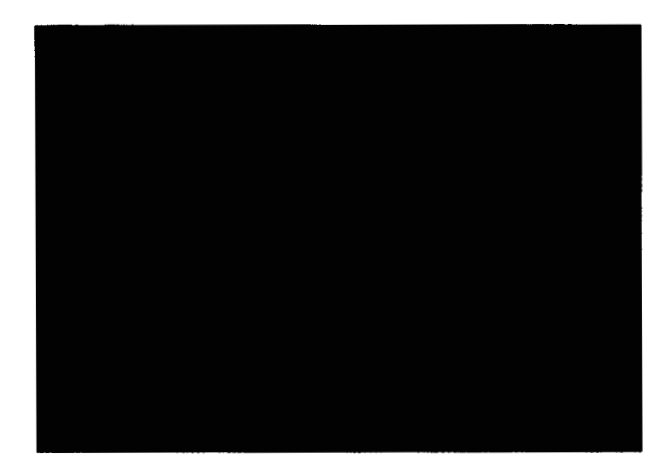


Figure 15

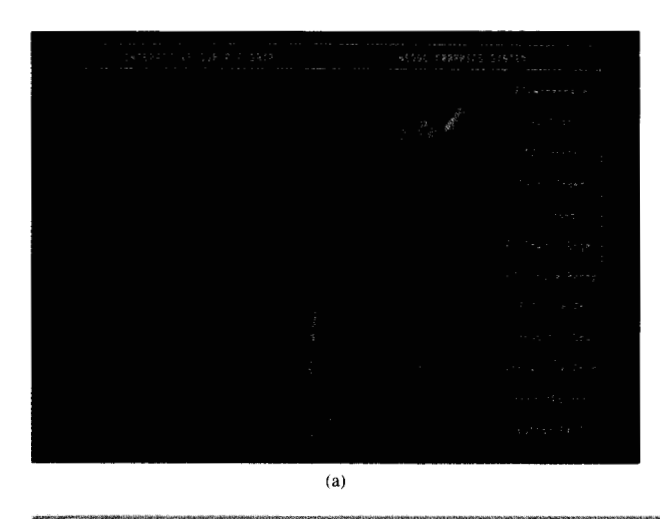
Cartesian surface mesh of total global ozone on October 10. 1986.

Figure 5 shows the basic daily TOMS grid as a simple Cartesian plot, and illustrates the nonuniformity of the grid structure as discussed earlier. It is critical to gain an understanding of the structure of the data prior to attempting more sophisticated visualizations. Figure 6 still deals with untransformed data for October 10, but these data now have been restructured. Although global mapping techniques are important for visualizing the spatial distribution of data across some geographic field, they may not be sufficiently quantitative at a detailed level for some applications. In other words, it is often useful to treat continuous or gridded data as scattered points, and vice versa. The pipeline is used to slice the ozone data into 10° latitude bands as an animation

sequence of 18 frames. The data from the second frame of this sequence (i.e.,  $-70^{\circ}$  to  $-80^{\circ}$  latitude) are plotted as a function of longitude. Specifically, the individual ozone cell values from that latitude band have been extracted from the world grid and are shown as a meridional distribution in this scatter diagram.

In order to focus on the ozone hole itself, transformation of the data must take place. In particular, several of the following examples concentrate on approximately the southern two-thirds of the Southern Hemisphere, Figure 7 shows the entire global distribution of the ozone grid on a Cartesian map (i.e., cylindrical equidistant projection). The scatter diagram is similar to the one in Figure 6. However, each point, as represented by a box, has been color-coded according to level of total ozone and displayed on a map. This technique is useful in understanding the actual (discrete) data distribution prior to further transformation or gridding that may alter that distribution. In addition to the actual grid structure. other artifacts of the observation process are also apparent as gaps in the data set. Figure 8 is the same representation as Figure 7, but uses an azimuthal equidistant map projection showing the desired portion of the Southern Hemisphere. This map projection and geographic window now begin to illustrate the spatial structure of the ozone hole, and the nonuniformity of the grid structure with respect to latitude is also visible.

Given an appropriate data transformation (i.e., the map projection), the data must be regridded according to that projection for use with a continuous visualization primitive. Different visualization primitives illustrate the characteristics of this transformed grid structure. In this case, the use of a continuous visualization primitive is required to impart spatial sense to the ozone hole



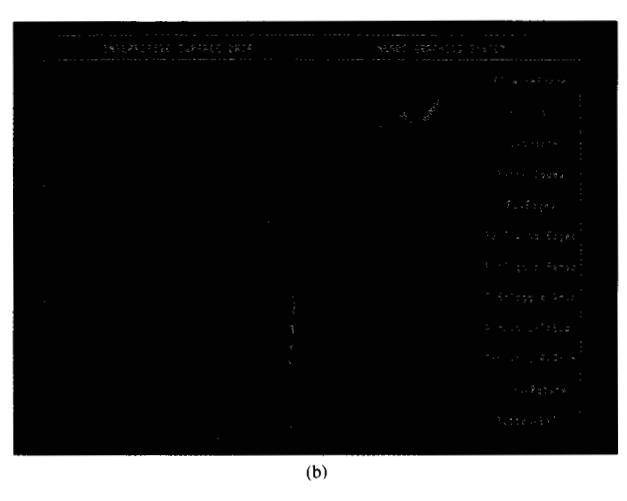


Figure 16

Gouraud-shaded Cartesian surface mesh (137 × 137) of total global ozone on October 10, 1986 (stereo pair).

structure. For these examples, a resolution of  $30 \times 30$ cells has been chosen. A nearest-neighbor algorithm, as described earlier, has been used to populate each cell of the grid with an ozone value. In other words, for any given cell in the  $30 \times 30$  grid, the value for ozone in the original grid structure spatially nearest to that cell has been chosen, after being transformed to an azimuthal equidistant map projection. The 30 × 30 (transformed) grid is rectangular and uniform so that each cell is a square. Figure 9 is a simple contour (iso-lines of total ozone in Dobson units) of that transformed grid with a world map overlay using the same geographic window as in Figure 8. Since the viewing window is in fact not a square, the grid resolution has been extended in the horizontal direction to preserve the uniformity of the grid. Hence, there are still 30 cells in the vertical direction. Figure 10 is a pseudo-color image of the same grid in the same window as in Figure 9. The pseudo-color spectrum (blue to red) has been mapped to a range of Dobson unit values. Although the geometric modeling in these visualization primitives is simple (the geographically transformed grid), it has been decoupled from the actual rendering as outlined above, since the same model has been used for both the contour and the image display. For this specific geographic window, the visualization as an image gives more information about the ozone hole structure than the contour plot.

The same grid or model can also be used to define a three-dimensional wire mesh, in which the third dimension corresponds to the total ozone. Such an "extension" of the model is shown in Figure 11. Figure 12 shows the surface as in Figure 11, except shaded with the same pseudo-color spectrum used in Figure 10. Such a height mapping begins to dramatize the concept of a hole in the ozone layer, while the layer enhances this perception as terrain color would improve a topographic map. However, this technique loses some of the quantitative detail available from other visualization techniques, which do not visually convey the hole as effectively.

Given the different visual characteristics of each of the continuous primitives shown so far, different gridding and even transformations may be required for an optimal display from each primitive. Figure 13 is a contour map like Figure 9, but showing a smaller area so that Antarctica fills the viewing window. Choosing the smaller geographic window eliminates the cluttering of contour lines and yields more effective quantitative information about the ozone distribution. The nominal grid used in this example consists of  $60 \times 60$  cells. The contour lines have been incremented every 20 Dobson units, and the statistics in this example are based upon the Southern Hemisphere data only. The yellow contour lines represent those values above one standard deviation

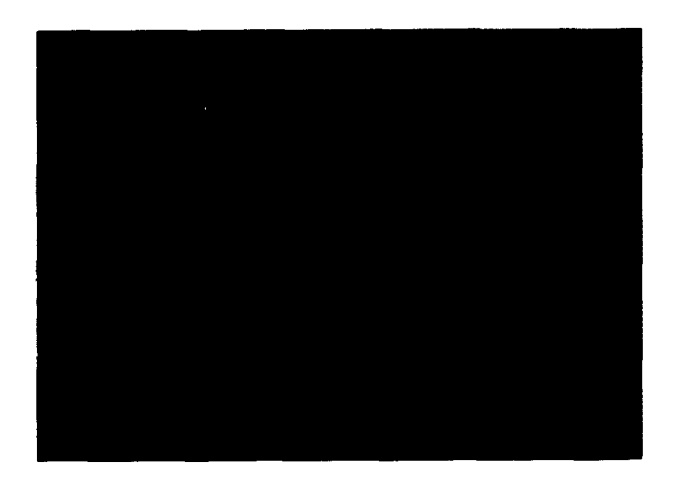


Figure 17

Geodesic wire-frame model (80 triangles) of total global ozone on October 10, 1986.

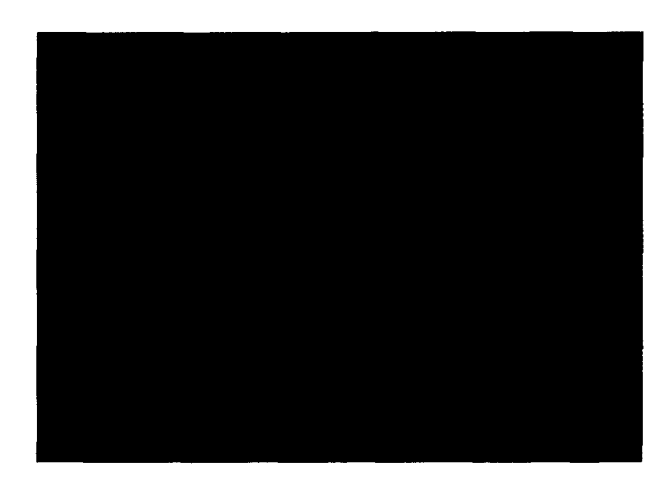
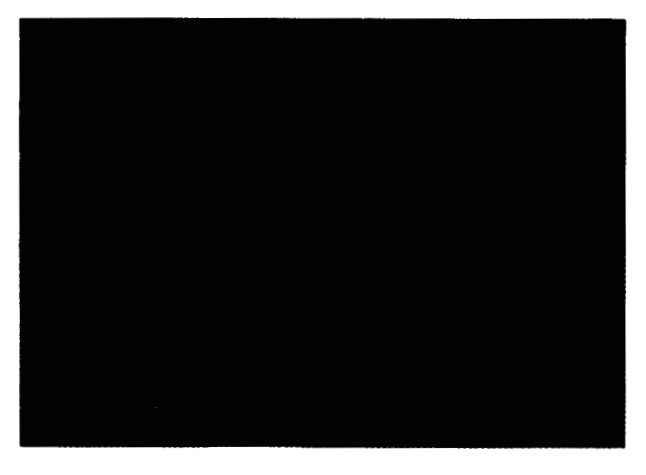


Figure 18

Geodesic shaded model (80 triangles) of total global ozone on October 10, 1986.

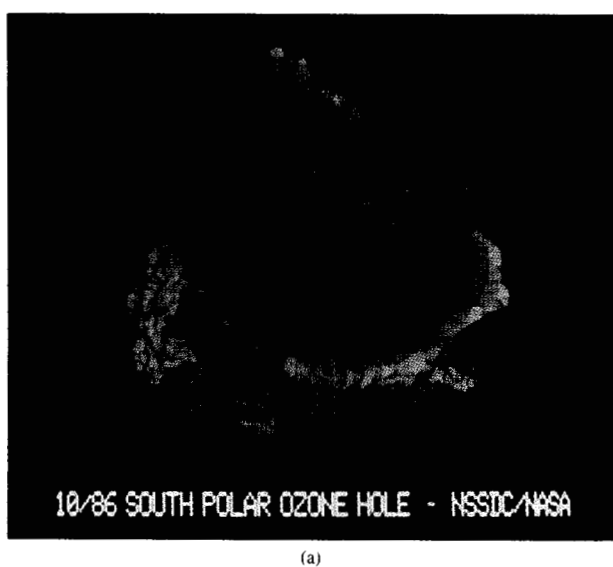
above the mean; the blue lines represent those values below one standard deviation below the mean; and the red lines cite intermediate values. This type of display shows the ozone hole structure with greater numeric precision than is possible with the pseudo-color image illustrated in **Figure 14**. This image utilizes a nominal grid of  $200 \times 200$  pixels and covers the same geographic region as do Figures 9 and 10. This presentation now shows the correlation between the ozone level and the coastlines. It should also be noted that the rendering time of the image was reduced by compressing the cell array via a quadtree as discussed earlier.

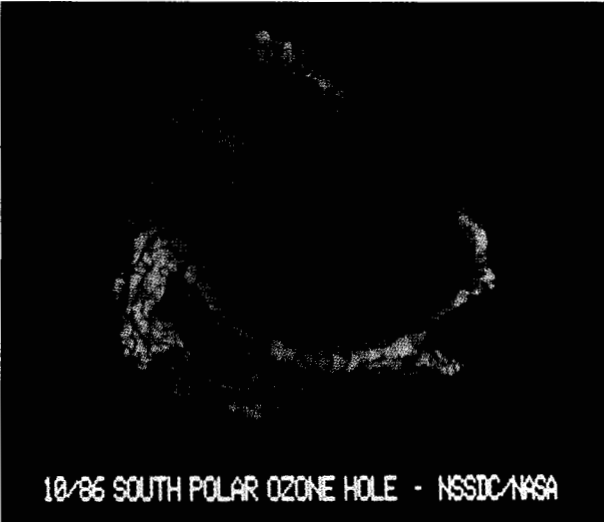


Geodesic wire-frame model (20480 triangles) of total global ozone over the South Pole on October 10, 1986.



Geodesic shaded model (20480 triangles) of total global ozone over the South Pole on October 10, 1986.





(b)

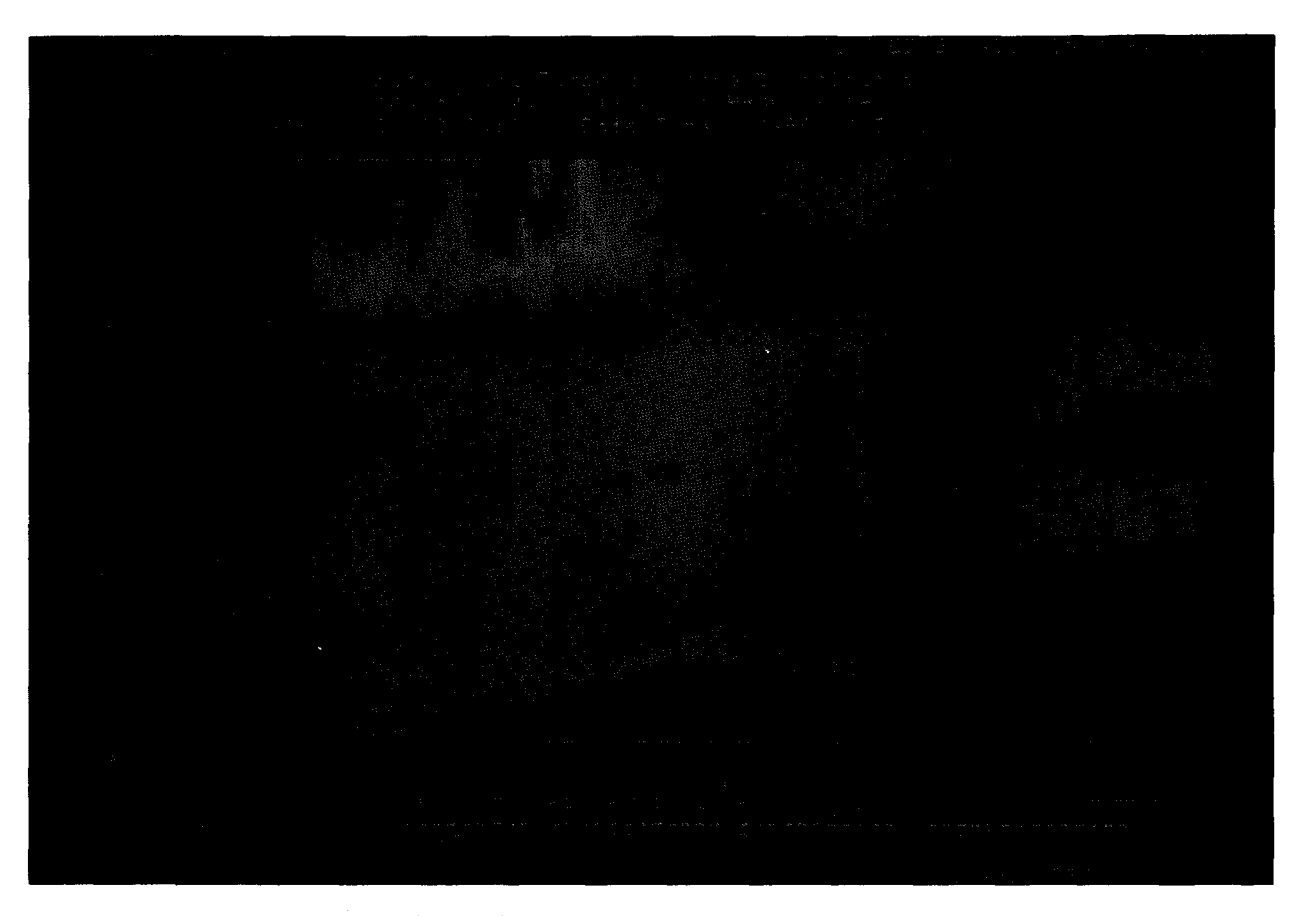
### Figure 21

Ray-traced rendering of geodesic model (81920 triangles) of total global ozone over the South Pole on October 10, 1986 (stereo pair).

A weighted-averaging algorithm, as described earlier, has been used to determine the ozone value for each cell in the grids used to generate Figures 13 and 14. In these cases, n = 3 nearest values for ozone have been chosen, after a transformation of the image to an azimuthal equidistant map projection. A weighting factor,  $w = d^{-2}$ , was computed after the data were transformed geographically. To reduce the computational time for the gridding, the data were projected into an octree.

Hierarchical search techniques sped up the time to search for the nearest three points to compute the weighted average for each cell in the final grid.

The technique used to generate the simple Cartesian surfaces in Figures 11 and 12 is a static one, which is limited to low-resolution meshes. In order to see more detail and view the data from different geographic perspectives, one must consider other rendering techniques, which can, for example, be enhanced in a



Finite 22

Pseudo-color image of the zonal distribution of Nimbus-7 TOMS total ozone in 1986.

framework operating on typical graphics devices with hardware support for three-dimensional graphics. Such devices permit interactive geometric transformations of surface meshes. Figures 15 through 20 were generated on systems from this class of graphics equipment supported by the NGS, namely the Megatek 9000 series of terminals via device-specific software. Since the rendering and modeling portions of the software are separate, a more modern and portable implementation of the rendering code has been recently completed using PHIGS+ on a Silicon Graphics Personal IRIS (4D/20).

Figure 15 shows a wire-frame representation with pseudo-coloring of the total ozone over the entire earth on October 10, 1986. The object, which consists of a 137 × 137 Cartesian mesh (18769 polygons), has been rotated in real time to show the ozone hole region on the right. This mesh has also been generated via a weighted-averaging algorithm. Figure 16 incorporates Gouraud shading of the mesh according to the same pseudo-color scheme. The ozone hole and adjacent ridge regions are visible in some detail on the right-hand side of the object,

which is further enhanced by the use of stereographic viewing.

As is apparent from the Cartesian displays in Figures 15 and 16, geographic data such as TOMS ozone statistics are obviously distorted when the inherently spherical geometry is ignored. Essentially, there is loss of geographic coherence in such a visualization technique. For two-dimensional visualization primitives. cartographic techniques, as illustrated above, solve the problem. However, in three dimensions a generic spherical geometry must be considered. For example, the ozone data can be modeled as a geodesic sphere by projecting the geographic data into an octree. For instance, a sphere which is deformed from a smooth sphere with a nominal radius according to the amount of total ozone can be used with a number of different renderers. Figures 17 through 21 are all rendered examples of such spherical models. In each case the radius and the color scale (blue to red) correspond to total ozone in Dobson units from 140 to 540, as with many of the preceding illustrations. To improve the

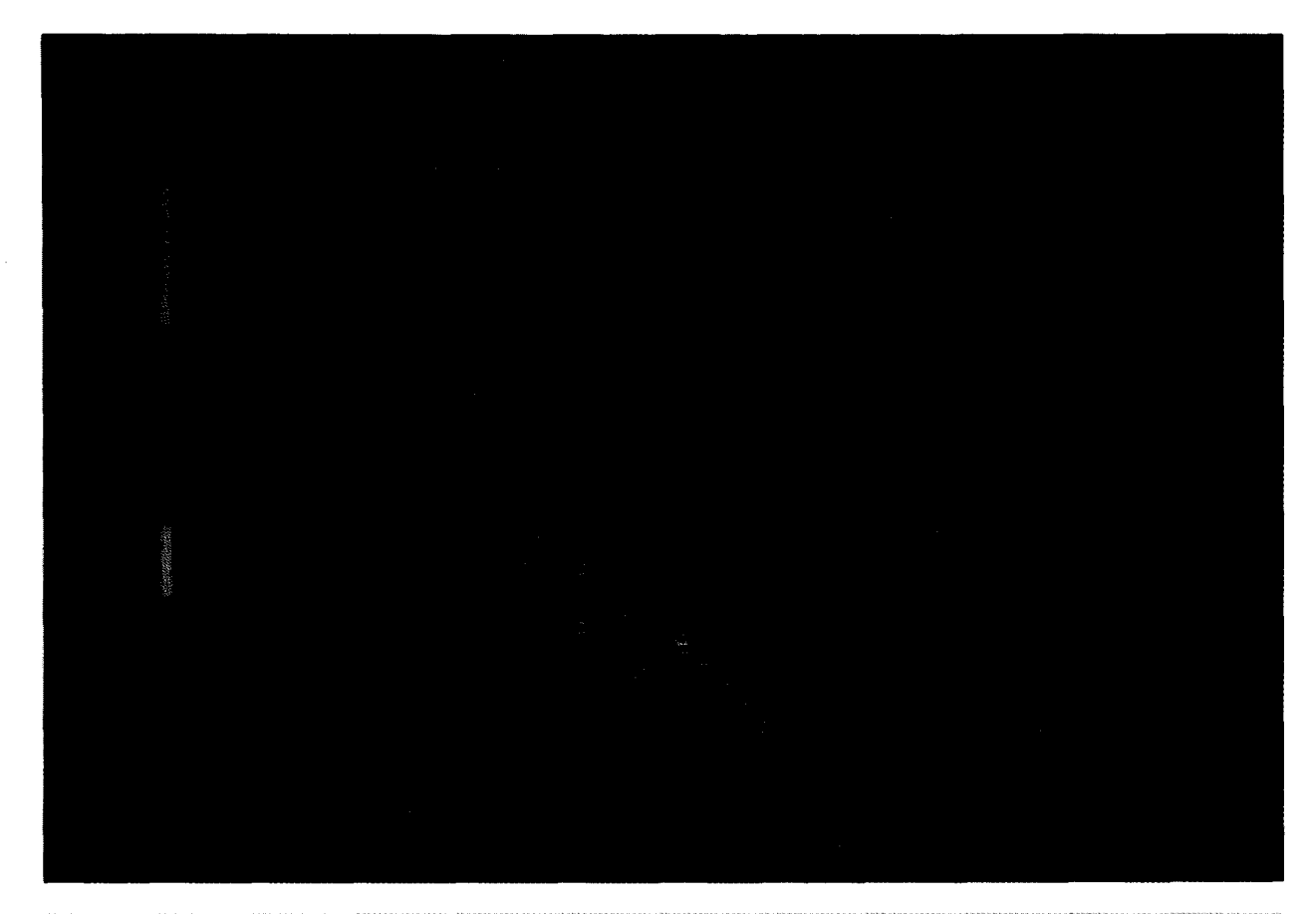


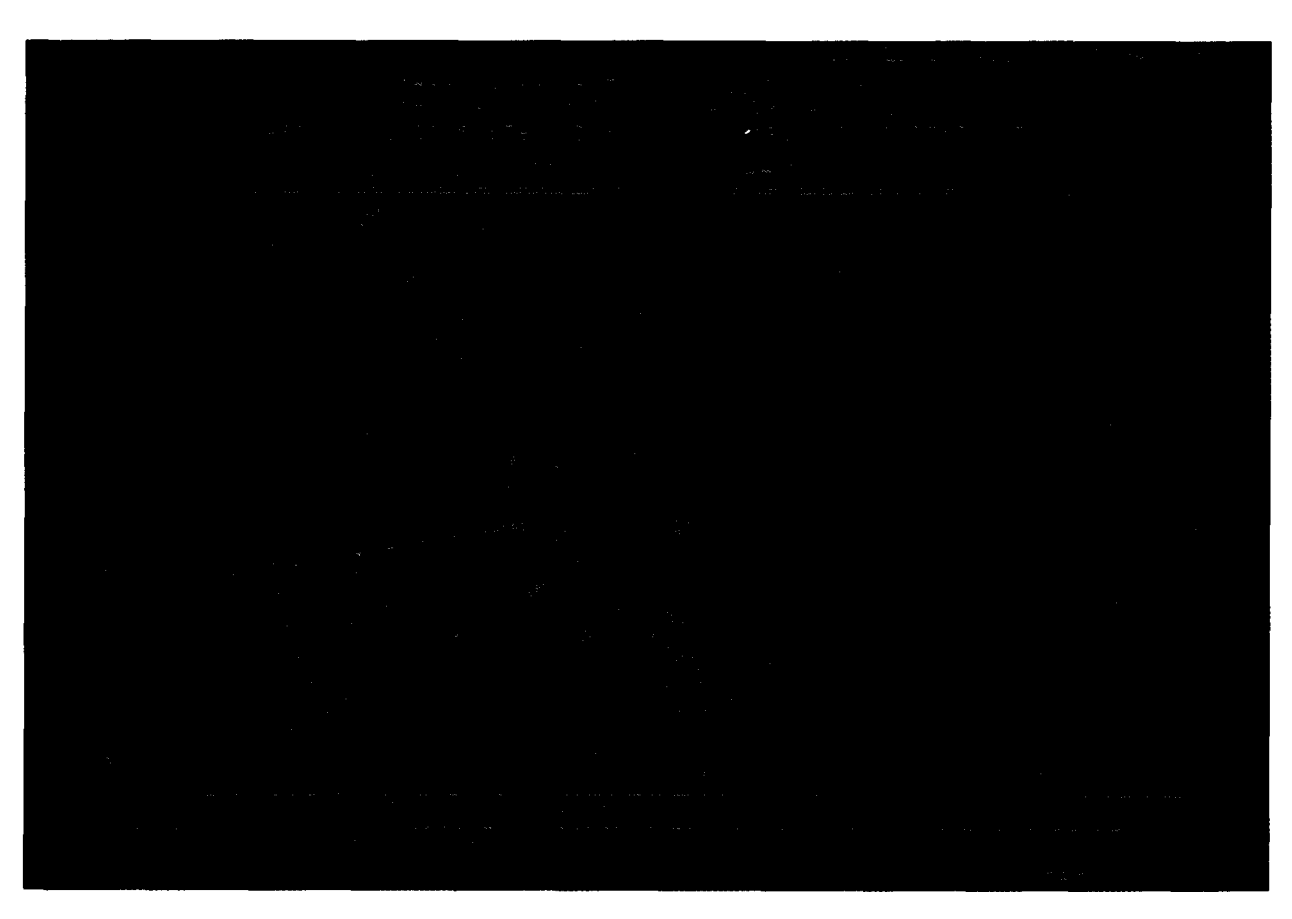
# Figure 23

Spatial distribution of Nimbus-7 SBUV total ozone over Antarctica on October 10, 1986.

quality and resolution of the resultant image, each model, which consists of a number of spherical triangles, can be further subdivided (e.g., each polygon gives birth to a new generation of smaller, connected polygons) at a cost in computation time. Thus, a given generation of subdivision has four times as many triangles as the previous generation and requires four times as much computation time.

Figure 17 shows the wire-frame mesh of the first generation (80 triangles) of the spherical geodesic. Figure 18 simply shows the model with flat, pseudo-color shading. Figures 19 and 20 show the results of subdividing four more generations (20480 triangles) in wire-frame and shaded renderings, respectively. In these cases, the objects have been rotated in real time to show the ozone hole. If the model is subdivided one more generation (81920 triangles), it can no longer be accommodated by the hardware renderer used to create Figures 17 through 20. In this case, a software ray-trace renderer has been used with the same geometric modeler, in which the casting of shadows helps to emphasize the spatial structure.

Figure 21 is an example of choosing such an expensive but high-quality presentation from the visualization pipeline. The view is directly over the South Pole with the prime meridian vertical. Other visualization techniques might emphasize only the detailed, quantitative nature of the spatial structure, as shown earlier. This technique emphasizes both qualitative and quantitative information about the total ozone. Since the ozone hole is quite prominent in the center, this particular picture has been dubbed the "ozone asteroid." The image achieves a better balance between spatial coherence and quantitative detail not present in other visualizations of these data. This effect is further enhanced by the use of stereographic viewing. The proper spatial relationship of the hole and ridge structure is illustrated (i.e., geographically as well as with respect to the data themselves—the ozone high appears to only partially fill the ozone hole). The color mapping was chosen to support simultaneously both pseudo-color spectrum scaling and shadowing, and to fit within an eight-bit frame buffer. Therefore, four bits are used for color and four bits are used for intensity.



Floure 24

Map of SBUV total ozone over Antarctica on October 10, 1986.

Figure 22 illustrates how the ozone hole data from October 10, 1986 relate to those from the rest of that year. Temporal and spatial considerations are shown by the zonal (i.e., by latitude) distribution of total ozone as a pseudo-color image over all of 1986. The nominal grid used for this image consists of 180 × 180 cells (i.e., each cell in the y-direction corresponds to one degree in latitude). A nearest-neighbor algorithm has been used to populate the latitude-time grid from the original volume of data. A summation of the evolution of the Antarctic ozone hole can easily be seen as the blue region near the bottom of the image, which begins to grow in September and dissipates in November. Portions of the image appear in black because of gaps in the observations that occurred when the TOMS instrument was not operating (e.g., during periods of local darkness during polar winter).

Despite the relative simplicity of this sample study of the TOMS ozone, it illustrates the power of an effective visualization pipeline. However, to indicate the value of such an approach for correlative data analysis, a few additional data sets are examined and then compared to the visual analysis of the TOMS data.

A major advantage of this class of techniques is, of course, their ability to support correlative data visualization. Nimbus-7 possesses another instrument which measures ozone, called the Solar Backscattered UltraViolet (SBUV) spectrophotometer. The SBUV observations are at a much lower global resolution than the TOMS data, and are available for the same time period as the TOMS data from the NSSDC. Rather than global grids, one of the SBUV data sets is organized as atmospheric profiles, in which measurements are available at different levels in the atmosphere along discrete orbital tracks. These profiles can be integrated to yield total ozone values [17]. The same geometric modeling and subsequent rendering techniques provided by the visualization pipeline can provide immediate visual correlation of these data sets. The SBUV total ozone data from October 10, 1986 are shown in Figure 23 over the Antarctic region using the data classification scheme employed in Figures 7 and 8 and the same

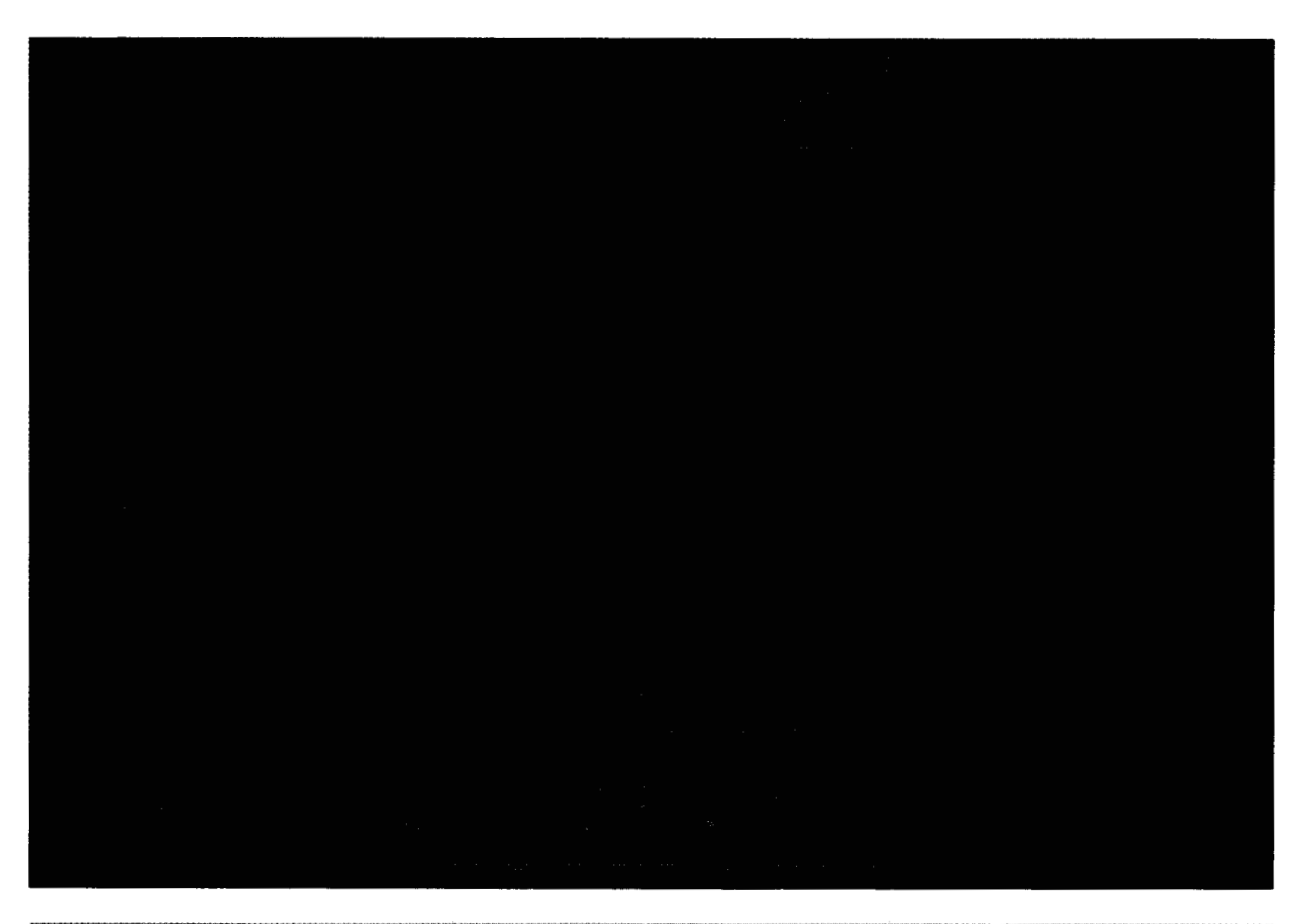


Figure 25

Meridional distribution of TOMS and SBUV total ozone from -60° to -90° latitude on October 10, 1986.

geographic window as in Figure 13. The individual tracks show the instrument's observation path via their respective orbital footprints. The discrete SBUV observations have been spatially integrated using the aforementioned weighted average octree technique to yield a transformed, interpolated grid with a nominal  $250 \times 250$  resolution. The grid has been rendered as the pseudo-color image in Figure 24. The result is a different visualization of the ozone hole than the one derived from the TOMS data. Artifacts of the gridding process are quite apparent, especially if the discrete data distribution is compared to the image. Despite that fact, the coarse geometric features in Figure 24 do correspond to those in Figures 13 and 14. To compare the SBUV and TOMS ozone data on a microscopic level, the October 10, 1986 data from each data set are displayed together. Figure 25 shows the meridional distribution of the polar data  $(-60^{\circ} \text{ to } -90^{\circ} \text{ latitude})$  by plotting TOMS total ozone (red squares) and SBUV total ozone (green circles) against common ozone and longitude scales. The key to the visual correlations between TOMS and SBUV data in Figures 24 and 25 is the ability of the scientist to display the data on common temporal and spatial bases.

To show that this approach can work with data that are not observations of the earth's ozone layer from NASA spacecraft, consider Figure 26, which is a pseudocolor image of the temperature of the earth's surface using the same geographic window as in Figure 14. This map is derived from a data set developed by the U.S. Navy Fleet Numerical Oceanography Center (FNOC), which is based upon 12-hour forecasts by the Navy's Operation Global Atmospheric Prediction System. FNOC has been accumulating the results of these numerical models, including many meteorological parameters, since the early 1960s. The scope of this data set has expanded in recent years to include, for example, global coverage every 12 hours since 1983 [18]. A nominal grid of 200 × 200 cells has been derived from the model-based global surface temperatures for October 10, 1986 at 00:00 GMT and displayed in Figure 26. No correlation between these data and the ozone data can be seen, which would be expected since the ozone values are

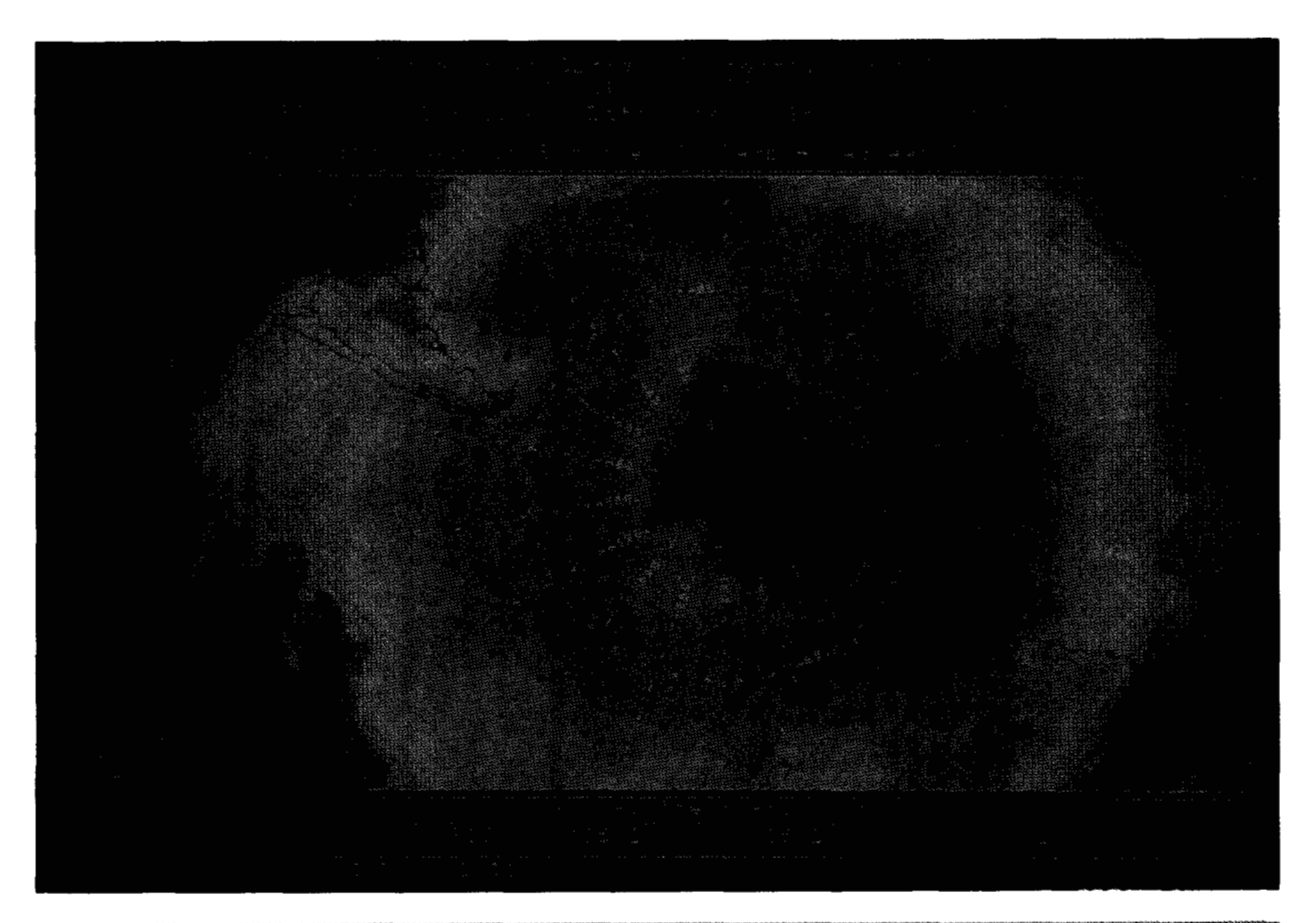


Figure 26

Map of FNOC model surface temperature on October 10, 1986, over the Southern Hemisphere.

derived from remotely sensed observations of the earth's stratosphere.

By having access to easy-to-use tools to reorganize data, a scientist can easily scrutinize the data at many different levels through disparate techniques. A profusion of visualization primitives properly coupled with powerful manipulation functions promotes the (visual) exploration of data and thus enables a scientist to extract knowledge from complex data.

# **Acknowledgments**

The research reported in this paper has been supported primarily by NASA's Office of Space Science and Applications (OSSA). The authors thank former members of the NSSDC staff, Michael Gough, Kuo-Piu Ni, and David Wildenhain, for significant contributions to this work. The authors also acknowledge James L. Green, Director of the NSSDC, for his continued support of the concept of discipline-independent software systems to support scientific research. In addition, the authors greatly appreciate the review of this manuscript by Robert Cromp.

#### References and notes

- B. K. McCormick, T. A. DeFanti, and M. D. Brown, "Visualization in Scientific Computing," *Comput. Graph.* 21, No. 6, 3 (November 1987).
- W. J. Campbell, N. M. Short, Jr., and L. A. Treinish, "Adding Intelligence to Scientific Data Management," *Comput. in Phys.* 3, No. 3 (May 1989).
- L. A. Treinish, "Discipline-Independent Data Visualization," Course No. 19: Visualization Techniques in the Physical Sciences, Fifteenth Conference of ACM SIGGRAPH, August 1988, pp. 119-207.
- L. A. Treinish and M. L. Gough, "A Software Package for the Data-Independent Storage of Multi-Dimensional Data," Eos Trans. Amer. Geophys. Union 68, No. 28, 633-635 (July 1987).
- M. Shaw, "Abstraction Techniques in Modern Programming Languages," *IEEE Software* 1, No. 4, 10–26 (October 1984).
- J. F. King, "Graphics Draw a New Picture for Science," Comput. in Phys. 1, No. 1, 50-57 (November-December 1987).
- L. A. Treinish, R. B. Haber, J. D. Foley, W. J. Campbell, and R. F. Gurwitz, "Effective Software Systems for Scientific Data Visualization," *Panel Session at the Sixteenth Conference of* ACM SIGGRAPH, August 3, 1989.
- T. A. DeFanti, "Cultural Roadblocks to Visualization," Comput. in Sci. 2, No. 1 (January 1988).
- L. A. Treinish, "An Interactive, Discipline-Independent Data Visualization System," Comput. in Phys. 3, No. 4 (July 1989).
- R. J. Renka, "Multivariate Interpolation of Large Sets of Scattered Data," ACM Trans. Math. Software 14, No. 2, 139– 148 (June 1988).

- D. Shepard, "A Two-Dimensional Interpolation Function for Irregularly-Spaced Data," *Proceedings of the 23rd National* ACM Conference, 1968, pp. 517–524.
- F. Pearson II, Map Projection Methods, Sigma Scientific, Inc., Blacksburg, VA, 1984.
- K.-P. Ni, M. L. Gough, and L. A. Treinish, "A Flexible, Template-Based Software Package for Generating Maps," 88-05 (February 1988), NSSDC, NASA/GSFC, Greenbelt, MD. This document can be acquired by contacting the National Space Science Data Center via internet, request@nssdca.gsfc.nasa.gov; SPAN, NSSDCA::Request; or telephone: 301-286-6695.
- H. Samet and R. E. Webber, "Hierarchical Structures and Algorithms for Computer Graphics Part I: Fundamentals," *IEEE Comput. Graph. & Appl.* 8, No. 3, 48-68 (May 1988).
- H. Samet and R. E. Webber, "Hierarchical Structures and Algorithms for Computer Graphics Part II: Applications, *IEEE Comput. Graph. & Appl.* 8, No. 4, 59–75 (July 1988).
- 16. A. J. Fleig, P. K. Bhartia, C. G. Wellemeyer, and D. S. Silberstein, "Seven Years of Total Ozone from the TOMS Instrument—A Report on Data Quality," Geophys. Res. Lett. 13, No. 12, 1355–1358 (November 1986). Much literature has been published on Nimbus-7 TOMS, which discusses the instrument and observations themselves, scientific interpretation and analysis of the TOMS data, and the morphology, structure, and evolution of global ozone, including the Antarctic ozone hole. For more information on this literature and related data sets and studies, a few of which are referenced in this paper, contact the user support office of the NASA Climate Data System at the National Space Science Data Center via internet, NCDSUSO@nssdca.gsfc.nasa.gov; SPAN, NSSDCA::NCDSUSO; or telephone: 301-286-5033.
- A. J. Fleig, P. K. Bhartia, and D. S. Silberstein, "An Assessment of the Long-Term Drift in SBUV Total Ozone Data," *Geophys. Res. Lett.* 13, No. 12, 1359–1362 (November 1986).
- Fleet Numerical Oceanography Center (FNOC). Meteorological and oceanographic models. FNOC Numerical Environmental Products Manual II, 1986, Commanding Officer, FNOC, Monterey, CA 93943.

Received November 17, 1989; accepted for publication October 30, 1990

Lloyd A. Treinish IBM Research Division, Thomas J. Watson Research Center, Yorktown Heights, New York 10598. Mr. Treinish is a research scientist at the IBM Thomas J. Watson Research Center in Yorktown Heights, New York. He works on techniques, architectures, and applications of data visualization for a wide variety of scientific disciplines. His research interests range from computer graphics, data storage structures, data representation methodologies, data base management, computer user interfaces, and data analysis algorithms to middle-atmosphere electrodynamics, planetary astronomy, and climatology. Mr. Treinish is particularly interested in generic or discipline-independent techniques for the storage, manipulation, analysis, and display of data. Earlier he did similar work in the development of advanced scientific data systems. including studying space and atmospheric phenomena, for over a decade at the National Space Science Data Center of NASA's Goddard Space Flight Center in Greenbelt, Maryland. A 1978 graduate of the Massachusetts Institute of Technology with an S.M. and an S.B. in physics, and an S.B. in earth and planetary sciences. Mr. Treinish has been at IBM since April 1990. He is a member of the IEEE Computer Society (IEEE-CS), the IEEE-CS Technical Committee on Computer Graphics, the Association for Computing Machinery (ACM), ACM SIGGRAPH, the National Computer Graphics Association, the Planetary Society, and the American Geophysical Union.